Pressure impulses during microsecond laser ablation

HanQun Shangguan, Lee W. Casperson, and Scott A. Prahl

The collapse of laser-induced cavitation bubbles creates acoustic transients within the surrounding medium and also pressure impulses to the ablation target and light-delivery fiber during microsecond laser ablation. The impulses are investigated here with time-resolved flash photography, and they are found to occur whether or not the light-delivery fiber is in contact with the target. We demonstrate that the impulses depend primarily on the energy stored in the cavitation bubble. They are not directly dependent on the mode of light delivery (contact versus noncontact), and they are also not directly correlated to the other acoustic transients. The pressure impulses do seem to be associated with the bubble-driven jet formation caused by the bubble collapse.

Key words: Cavitation, laser thrombolysis, laser ablation.

1. Introduction

It is well known that cavitation can occur when a sufficiently intense light pulse is delivered to an absorbing liquid or to an absorbing target within a liquid. This cavitation can be caused by tensile stress, plasma formation, or vaporization, and it typically results in bubble formation and acoustic transients.[1–4] For the medical applications of interest here, the laser energy is absorbed by thrombus (blood clot) in an obstructed artery. The bubble expansion and subsequent collapse act to destroy the thrombus with minimal damage to the surrounding tissue. This form of therapy has been termed laser thrombolysis.[5] During the therapy, laser pulses are delivered to the blood clot by an optical fiber. The light-delivery fiber may or may not be in direct contact with the target to be ablated.[5–7] The ablation process is profoundly affected by these two modalities, and the contact ablation efficiency may be at least 3 times greater than the noncontact ablation efficiency.[8] The mass ablated is correlated with the acoustic pressure of the cavitation bubble, and the acoustic signals can be used as a means to estimate the ablation efficiency as well.[8,9]

In experimental simulations, pressure impulses follow the laser pulse and sometimes are found to cause vertical displacement of the cuvette containing the ablation targets.[10] The displacement is proportional to the bubble size regardless of the light-delivery method (contact versus noncontact), although the mode of light delivery significantly affects the generation of the acoustic transients.[8] For example, the acoustic pressures generated by contact delivery are similar to those during noncontact delivery at 3 times the pulse energy.

This study has been motivated by two concerns: (1) Does the internal acoustic pressure correlate with the generation of the pressure impulses that displace the cuvette? (That is, can the acoustic signal be used as a tool to estimate the pressure-impulse generation?) (2) Could the pressure impulses cause tissue motion such that the catheter would penetrate the walls of a blood vessel during laser thrombolysis? Previous studies of laser-induced pressure waves have focused on the effects of the laser energy, pulse duration, absorption coefficient, fiber size, and material strength on the acoustic pressure generation.[1,3,11] The acoustic pressure waves are detected in the early expansion phase and in the subsequent collapse phase of the bubble evolution. At modest irradiance levels where dielectric breakdown is absent, two mechanisms of stress wave generation, thermal-elastic effect and ablative recoil, have been proposed.[3] However, the physical mechanism of the pressure-impulse generation during microsecond laser ablation has not been previously studied.

Pulsed laser ablation above threshold in a blood-

H.-Q. Shangguan and S. A. Prahl are with the Oregon Medical Laser Center, 9205 SW Barnes Road, Portland, Oregon 97225. S. A. Prahl is also with the Oregon Health Sciences University, Portland, Oregon 97201. L. W. Casperson is with The Institute of Optics, University of Rochester, Rochester, New York 14627 and the Department of Electrical Engineering, Portland State University, Portland, Oregon 97207.

Received 2 April 1997; revised manuscript received 29 July 1997.
0003-6935/97/349034-08$10.00/0

filled vessel is always accompanied by cavitation. The mechanical effects of the cavitation bubble formation have been proposed to be potential damage mechanisms during laser angioplasty.[11–13] van Leeuwen *et al*. demonstrated that the expansion and collapse of a cavitation bubble caused a microsecond dilatation of the femoral and iliac artery followed by a microsecond invagination of the artery in a rabbit model.[13] The extensive damage to the adjacent arterial wall was also observed after excimer laser angioplasty. It is possible that the collapsing bubble in combination with friction between the arterial wall and the edge of the catheter tip tears the internal elastic lamina from the wall. Thus the mechanical effects of the pressure impulses that may occur in laser thrombolysis are of substantial clinical interest.

The major goal of this study was to investigate the mechanism of the pressure-impulse generation during contact and noncontact ablation. The impulses were quantitatively estimated through measuring the change in momentum of the cuvette before and after laser irradiation. The ablation process was visualized by using time-resolved flash photography. The strength of the potentially damaging impulses that have sometimes been observed depends on the energy stored in the cavitation bubble regardless of the light-delivery method (contact versus noncontact). The bubble-driven jet formation does seem to be associated with the impulses. In addition, we investigated the mechanical effects of the resulting pressure impulses by changing boundary conditions, and it was also found that the impulses depend sensitively on the manner in which an *in vitro* experiment is configured. The results may have clinical implications for laser thrombolysis.

2. Materials and Methods

A. Pressure-Impulse Generation

1. Theory

The pressure impulses were estimated by measuring the change in momentum of a cuvette containing the target medium resulting from the laser pulses during contact and noncontact ablation. The impulse $\mathbf{I}$ is a vector defined by[14]

$$\mathbf{I} = \int_{t_i}^{t_f} \mathbf{F}\,\mathrm{d}t, \tag{1}$$

where $\mathbf{F}$ is the net force that causes the displacement of the cuvette and t_i and t_f are the times before and after the force.

According to Newton's second law $\mathbf{F} = \mathbf{dP}/\mathrm{d}t$, we can see that the impulse equals the change in momentum during the time interval:

$$\mathbf{I} = \int_{t_i}^{t_f} \mathbf{F}\,\mathrm{d}t = \int_{t_i}^{t_f} \frac{\mathbf{dP}}{\mathrm{d}t}\,\mathrm{d}t = \mathbf{P}_f - \mathbf{P}_i = m\mathbf{v}_f - m\mathbf{v}_i, \tag{2}$$

where $\mathbf{P}_i$ and $\mathbf{P}_f$ are the initial and the final momentum of the cuvette, respectively, m is the mass of the cuvette, and $\mathbf{v}_i$ and $\mathbf{v}_f$ are the initial velocity of the cuvette (i.e., zero) and the final velocity (takeoff velocity), respectively.

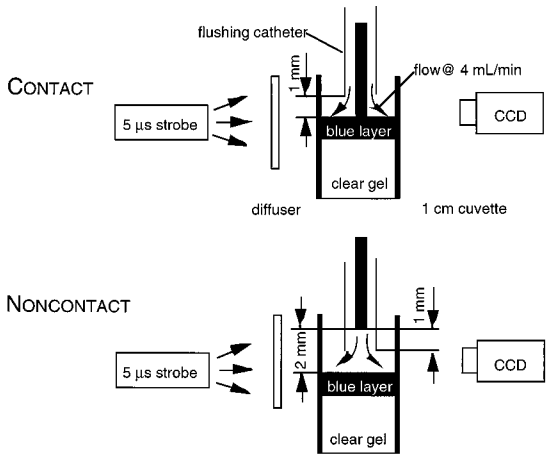

Fig. 1. Schematic illustration of two ablation configurations (contact and noncontact delivery) for cuvette experiments.

The pulses were incident on the target from above as shown in Fig. 1, and the cuvette was found to move upward after the laser pulses. Based on conservation of energy, we obtain

$$mgh_{\max} = \tfrac{1}{2}mv_f^2, \tag{3}$$

where g is the acceleration of gravity and $h_{\max}$ is the maximum height reached by the cuvette. The value of $h_{\max}$ was measured by using time-resolved flash photography (Fig. 2). By substituting Eq. (3) into Eq. (2), we can estimate the impulse generated by the laser pulse by

$$I = mv_f = m\sqrt{2gh_{\max}}. \tag{4}$$

The pressure impulse is equal to this impulse divided by the area S of the interface between the cuvette and the metal plate, i.e.,

$$I_{\text{pressure}} = m\sqrt{2gh_{\max}}/S. \tag{5}$$

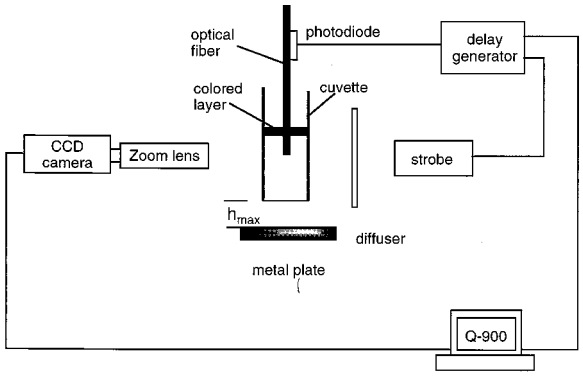

Fig. 2. Experimental setup for time-resolved flash photography of the effects of pressure impulses on ablation targets during microsecond laser ablation.

2. Experiments

The experiments were performed by changing (1) radiant exposure and (2) laser-pulse energy for addressing two concerns: (a) Is the impulse dependent on the radiant exposure or the laser-pulse energy? (b) How does the light-delivery method affect the impulses? First, single pulses of 20 mJ were delivered through a flushing catheter onto gelatin samples under distilled water for contact delivery, while single pulses of 60 mJ were used for noncontact delivery, as shown in Fig. 1. The catheter consisted of a step-index fused-silica optical fiber contained inside a 1-mm flexible Teflon tube. The core diameter was varied between 200 and 400 μm. The fiber tip extended 1 mm from the distal end of the catheter during contact delivery; the tip was 1 mm inside the catheter during noncontact. The spot sizes on the ablation targets were obtained from the burn pattern on a deep-dyed polyester film: 200, 300, and 400 μm for contact ablation and 450, 480, and 520 μm for noncontact. In a second series of experiments we measured the displacement by changing the laser energy delivered by way of the flushing catheter with a single 300-μm fiber. Contact experiments used 15, 20, and 25 mJ/pulse, respectively; noncontact experiments used 3 times as much.

In both experiments, distilled water was injected through the Teflon tube with a syringe infusion pump (Harvard apparatus) at a flow rate of 4 ml/min to wash away the removed gelatin from the target site. The flow was stopped immediately after the laser pulse. The mass in Eq. (5) was determined by weighing the cuvette containing the gelatin sample and water after ablation to ensure that the weight for each experiment was similar. The typical weight was ~6 g for each experiment. The cuvette was placed loosely on a metal plate, and the catheter was fixed, which made it possible to estimate the pressure impulses through measuring the rebound. Otherwise, a soft boundary would absorb the momentum. The maximum height was determined by directly measuring the image of the cuvette while varying the delay time between the end of the laser pulse and the height-recording strobe flash. This delay time aspect of the experimental setup is shown in more detail in Fig. 2, and a description of this setup has also been previously given.[10]

B. Cavitation Bubble Dynamics

Cavitation bubble formation is a major event occurring during laser thrombolysis, and the displacement of the cuvette is proportional to the bubble size.[10] To understand the physics behind the experimental observations we correlated the pressure impulses with the total energy of the cavitation bubble. For simplicity, Rayleigh's formulas[15,16] were used to estimate the bubble energy by assuming that the bubble has a spherical geometry and is filled only with vapor in an infinite and incompressible liquid without the effects of viscosity. The total energy of the cavitation bubble E_B is given by

$$E_B = \tfrac{4}{3}\pi {R_{\max}}^3 \Delta p, \tag{6}$$

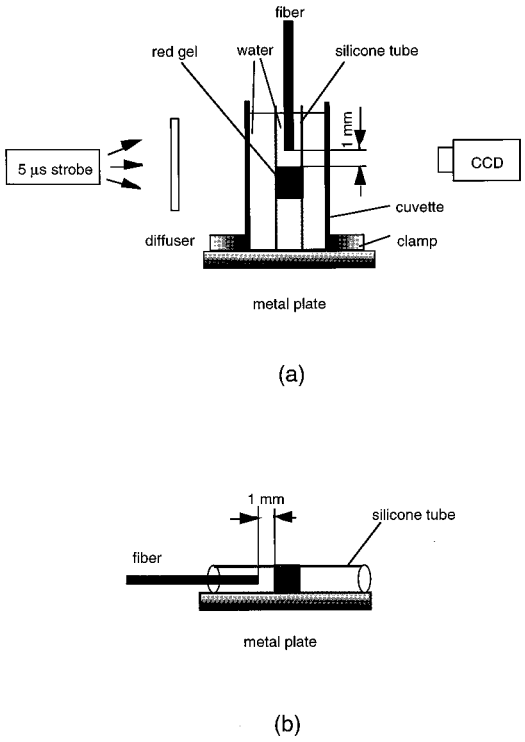

Fig. 3. Schematic illustration of two ablation configurations for tube experiments (noncontact) (a) vertically submerged in a 1-cm cuvette filled with water and (b) loosely laid on the metal plate.

where $R_{\max}$ is the maximum bubble radius and Δp is the difference between inner and outer pressure. In this study the difference was assumed to be close to 0.1 MPa (the hydrostatic pressure). The bubble formation was visualized with the flash photographic setup shown in Fig. 2.

C. Mechanical Effects of Pressure Impulses

Two experimental protocols were employed to investigate qualitatively the mechanical effects of the pressure impulses on ablation targets with different experimental configurations. No attempt was made to compare quantitatively any differences for each experiment. First, the cuvette was suspended using a rubber ring, so that the cuvette did not contact the metal plate. The purpose of this experiment was to investigate the effect of the impulse on an unbounded cuvette. This experiment used the same laser parameters as those used in the experiment in Subsection 2.A. To simulate cardiovascular applications, in the second experiment, single laser pulses of 60 mJ were delivered by way of a 300-μm fiber onto gelatin samples confined in silicone tubes (45 mm long with an inner diameter of 3 mm and a wall thickness of 0.4 mm). The weight of the tubes containing gelatin and water was ~0.4 g. The tubes were either vertically submerged in a 1-cm cuvette filled with water [Fig. 3(a)] or loosely laid on the metal plate [Fig. 3(b)]. The cuvette containing the tube was firmly fixed on the metal plate with a metal clamp. In both experiments the position of the cuvette or tube was also

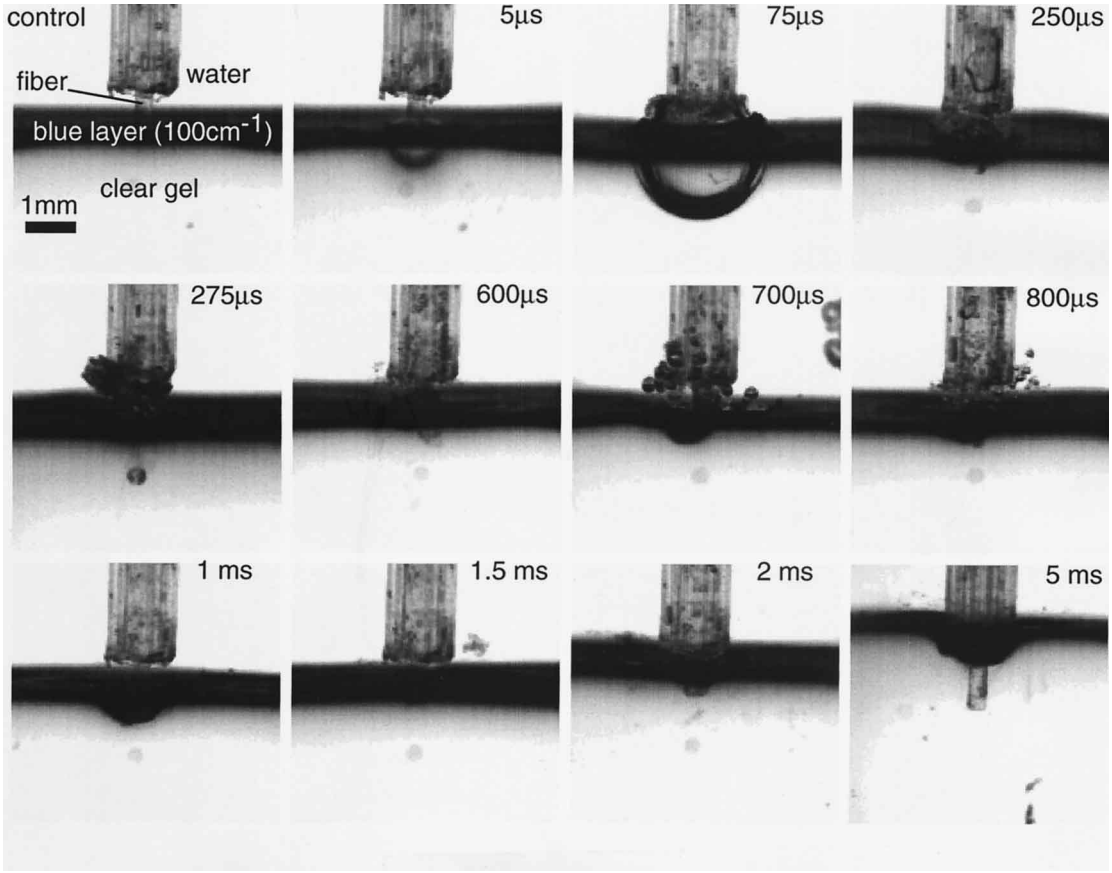

Fig. 4. Bubble formation on gelatin when the optical fiber is in contact with the gelatin surface. The optical fiber is centered in a 1-cm cuvette. A single pulse of 20-mJ laser energy was delivered through a flushing catheter with a 300-μm-diameter fiber. The colored layer was 300 μm thick but appears thicker because of a slight curvature of the surface.

monitored with the flash photographic setup shown in Fig. 2.

D. Ablation Targets

The targets for the cuvette experiments were 3.5% 175 bloom gelatin (Sigma) containing Blue 15 dye or Direct Red 81 (Sigma) as the chromophore. The percentage was determined by the weight ratio of gelatin to water. The bloom number is the standard method for indicating the toughness of gelatin and is a measure of surface tension. Higher bloom numbers represent stronger gelatin. The gelatin–water mixture was heated to 60 °C with stirring until it became clear. The clear liquid gelatin was poured in 1-cm cuvettes and cured to form 2–3-cm-thick targets with flat surfaces. A dye solution (0.07 g of Blue 15 or 0.089 g of Direct Red 81 in 40 ml of water) was placed on the gelatin surface for 5 min, and a blue/red layer ~300 μm thick with an absorption coefficient of ~100 cm^{-1} at 577 nm/504 nm was formed. This colored layer served as a phantom for the thrombus targets that might occur in medical applications and also allowed the boundaries of the cavitation bubble to be visible, even when they otherwise would been hidden by a light-absorbing gelatin substrate (Fig. 1).

The targets for the tube experiments were made by adding 1.2 g of Direct Red 81 into 100 ml of the 3.5% 175 bloom clear liquid gelatin. The absorption coefficient was ~100 cm^{-1} at 504 nm. The colored liquid gels were drawn into the 3-mm silicone tubes and allowed to cure.

E. Laser System

The samples were irradiated by a flashlamp-excited dye laser (Palomar Medical Technologies), and the experiments were performed at the wavelengths of 577 or 504 nm. The laser-pulse duration was ~1.3 μs (full width at half-maximum). The energy per pulse was measured with a joulemeter (Molectron), and pulse-to-pulse energy variation was less than 5%.

3. Results

A. Bubble Formation

The characteristic evolutions of laser-induced cavitation bubbles during contact and noncontact ablation are presented in Figs. 4 and 5, respectively. Evidently, a laser pulse generated a cavitation bubble either at the fiber tip or on the gelatin surface depending on where the laser light was absorbed. Each picture was a single event and was repeated 3 times for each sample. The imaging times extend from 10 μs to 2 ms for contact delivery and from 10 μs

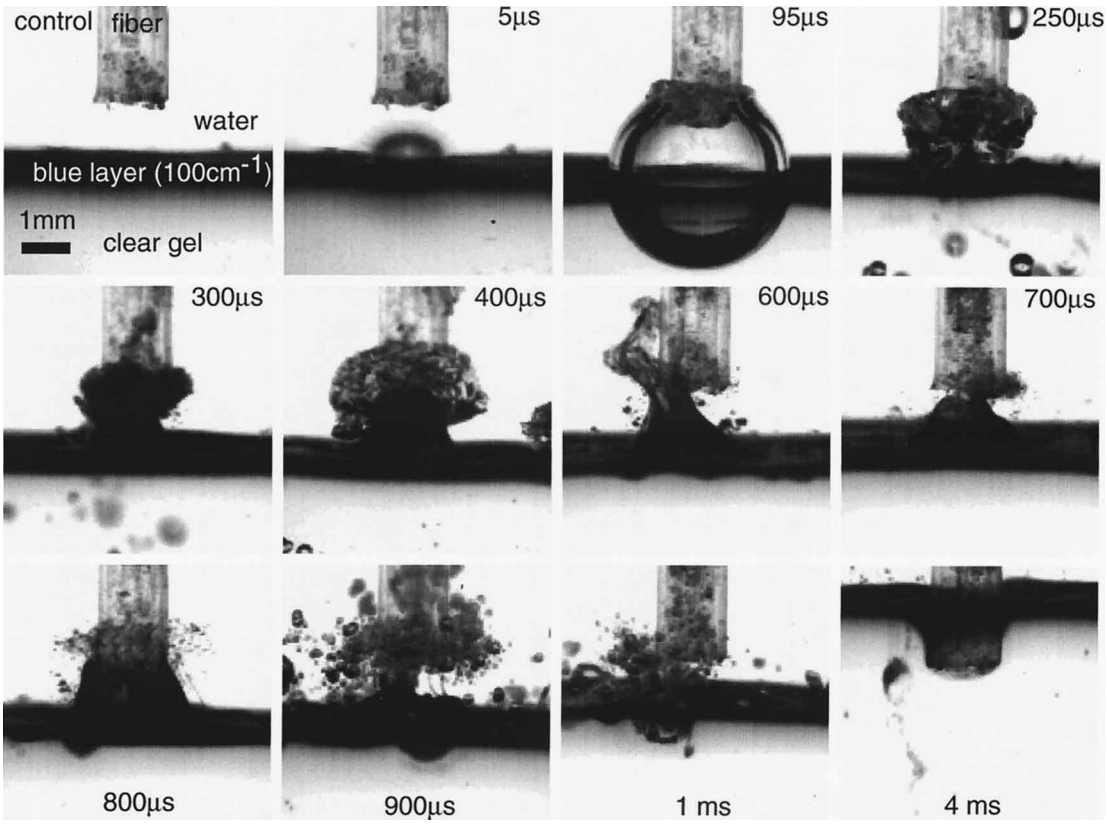

Fig. 5. Bubble formation on gelatin when the optical fiber is 2 mm above the gelatin surface. The optical fiber is centered in a 1-cm cuvette. A single 60-mJ laser pulse was delivered through a flushing catheter with a 300-μm-diameter fiber. The colored layer was 300 μm thick.

to 20 ms for noncontact delivery. The bubble size was fairly reproducible during the bubble expansion, whereas the appearance of the cavitation bubbles varied widely during the bubble collapse.

A compilation of the bubble expansion and collapse sequence for contact ablation is presented in Fig. 4. The imaged bubbles were formed after laser irradiation with single pulses of 20 mJ delivered by a flushing catheter with a 300-μm fiber. The maximum width of the bubble was ~2.8 mm at 75 μs. The bubble completely collapsed 250 μs after the laser pulse. Significant ejection of colored gelatin moving away from the surface was observed at 275 and 700 μs, respectively. The displacement of the cuvette was observed at ~800 μs. The exact elevation time was difficult to image with this technique. The maximum displacement was ~1.8 mm and was reached at 2 ms after the laser pulse.

The bubble evolution for noncontact ablation using single pulses of 60 mJ delivered by the flushing catheter with a 300-μm fiber is shown in Fig. 5. The maximum width of the bubble was measured as 3.6 mm at 95 μs. The bubble completely collapsed ~300 μs after the laser pulse, and the ejection of the gelatin started afterward. The movement of the cuvette was observed at ~700 μs. The cuvette reached its maximum height of ~5.5 mm at ~20 ms after the laser pulse (not shown in Fig. 5 because the image could not be represented to the same scale as the rest). In both cases, no movement of the cuvette could be seen before the material ejection occurred. The bubble sizes generated by contact delivery were always greater than those generated by noncontact delivery when the same energy was used; e.g., a single pulse of 20 mJ generated a bubble of 2.8 mm in diameter by contact delivery but only ~1.8 mm for noncontact delivery.

B. Effects of Radiant Exposure and Laser Pulse Energy on Pressure Impulses

The pressure impulses of the cuvettes containing the ablation targets were estimated by using Eq. (5). Figure 6 shows the pressure impulse as a function of radiant exposure. The impulses are seen to be independent of the radiant exposure. There were no significant differences in the impulses at different spot sizes for either contact ablation or noncontact ablation when the same laser energies were used.

The relation between the laser-pulse energy and bubble energy is represented in Fig. 7. The bubble energies were calculated with Eq. (6). The efficiency by which laser energy is converted into bubble energy can be read from the slope of the straight lines. It is 6% for contact delivery and 4% for noncontact delivery. Figure 8 shows the pressure impulse as a function of the corresponding bubble energy. Unlike the acoustic pressure waves, the pressure impulses primarily depended on the bubble energy regardless of the light-delivery method. An almost linear relation

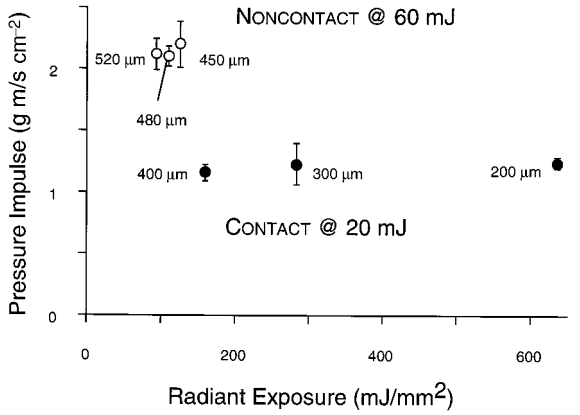

Fig. 6. Pressure impulse as a function of radiant exposure. Open circles represent the noncontact delivery, and solid circles represent the contact data. The flushing catheter with a 200–400-μm fiber was used for the light delivery. The spot sizes are labeled. Error bars represent the standard deviation of five measurements.

between the bubble energy and pressure impulse seems to exist.

C. Mechanical Effects of Pressure Impulses

No displacement of the cuvette was observed when the cuvette did not contact the metal plate. It was also observed that the displacement of the cuvette decreased dramatically when a soft material, e.g., tissue paper, was put between the bottom of the cuvette and the metal plate. Similar effects were observed during the tube experiments. However, the surface of the water contained in the cuvette vibrated in each experiment.

The results of the tube experiments revealed that a single laser pulse of 60 mJ could cause the tube submerged in a 1-cm cuvette to jump more than 2 mm at 5 ms after the laser pulse while the cuvette remained static and that such a pulse could also cause the tube to jump as high as 0.5 mm when it was loosely laid on the metal plate. No displacement of the tubes was observed when wet tissue paper (>5 mm thick) was placed underneath the tube or cuvette in the two cases.

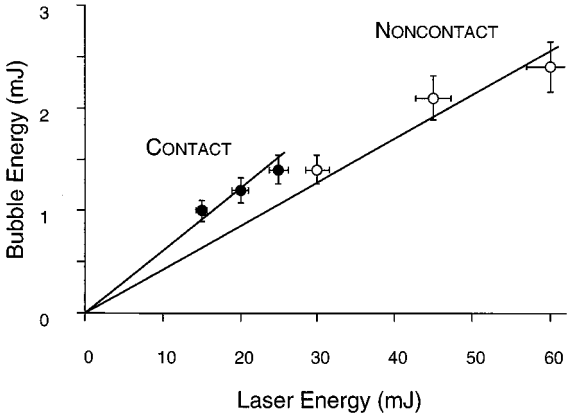

Fig. 7. Cavitation bubble energy as a function of the laser-pulse energy. Open circles represent the noncontact delivery, and solid circles represent the contact data. The flushing catheter with a 300-μm fiber was used for the light delivery. Error bars represent the standard deviation of five measurements.

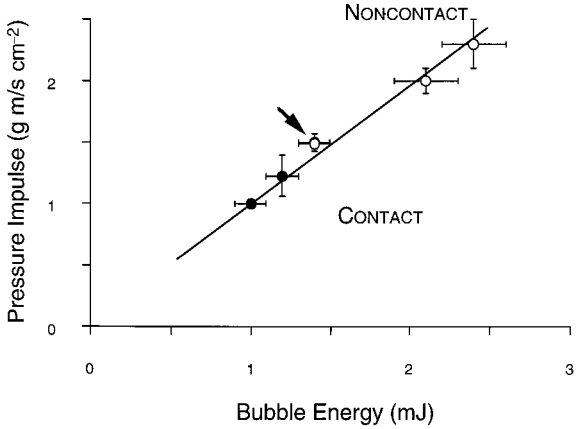

Fig. 8. Pressure impulse as a function of bubble energy. Open circles represent the noncontact delivery, and solid circles represent the contact data. The flushing catheter with a 300-μm fiber was used for the light delivery. The arrow indicates two overlapped data points. Error bars represent the standard deviation of five measurements.

4. Discussion

In this study we have used a simple method to estimate quantitatively the pressure impulses generated by microsecond laser pulses during contact and noncontact ablation. This method is based on the change in the momentum of the cuvette containing the ablation target and allows the mechanism of the pressure-impulse generation and mechanical effects of the resulting impulses to be investigated. A gelatin-based thrombus model was used as the ablation target and was ablated under water with different boundary conditions, and the results may have clinical implications for laser thrombolysis.

The sequence of events occurring during laser thrombolysis with contact and noncontact delivery is almost the same: cavitation bubble formation, material ejection, and pressure-impulse generation. The photographs reveal that (1) the bubble formation was a major and inescapable process, (2) ejection of colored gelatin into the water side followed the bubble collapse, and (3) no displacement was observed before the material ejection. The similarities of the experimental observations suggest that the mechanism of the pressure-impulse generation involved in both cases is possibly the same, although contact and noncontact ablations differ in a few ways.[8]

As shown in Figs. 4 and 5, the laser-induced cavitation bubble grows to a maximal size and then collapses on itself some hundreds of microseconds later. Like laser lithotripsy,[2] pressure waves generated during the expansion and collapse of the bubble induce mechanical stresses within the gelatin sample. The gelatin layer is ejected into the water for a distance of several millimeters by stress exceeding its tensile strength. Previous studies have demonstrated that a high-speed liquid jet directed toward a

boundary is generated when a bubble collapses in the vicinity of that boundary due to a Kelvin impulse.[17,18] The Kelvin impulse can be regarded as linear momentum of the bubble if a virtual mass induced by the fluid motion is attributed to the cavity. In this study a jet of gelatin then moves toward the water side, presumably as a result of boundary effects: (1) symmetrical geometry in the radial direction, which prevents the jet from moving radially, and (2) resistance asymmetry in the axial direction at the interface between the gelatin and water, which leads the ejected material toward the water side where less resistance exists compared to the gelatin side. The bubble also delivers an impulse to the gel surface because of conservation of momentum. The impulse propagates down to the bottom of the cuvette, and then it is reflected from the metal plate because of the impedance mismatch. Eventually, the reflected pressure causes the displacement of the cuvette. Thus the pressure impulses could be quantitatively estimated through measuring the change in the momentum of the cuvette before and after the laser irradiation. We hypothesize that the bubble-driven jet formation is closely associated with the pressure-impulse generation during contact and noncontact ablation. A recent study by Chapyak *et al*. also numerically demonstrated that a collapsing bubble could generate jetting in both axial directions due to the dissipative mechanisms during noncontact ablation.[19] Moreover, we observed that fractures were formed underneath the craters in some samples after laser irradiation, which might be caused by the jet penetration into gelatin as well.

The pressure impulses primarily depend on the bubble energy and are not directly dependent on the mode of the light delivery (Fig. 8). Thus a cavitation bubble 3 mm in diameter generated by either 25 mJ when contact delivery is used or 30 mJ when noncontact delivery is used could produce a similar pressure impulse. However, a 20-mJ pulse could cause a cuvette of 6 g to rebound 1.8 mm when contact delivery is used but less than 1 mm when noncontact delivery is used. These pressure-impulse observations are in contrast to the previously described effect of delivery mode on the amplitude of acoustic pressure waves,[8] and the relation between the light-delivery method and the pressure impulse seems to be quite complicated. The results shown in Fig. 6 indicate that the pressure impulses depend on the laser-pulse energy rather than the radiant exposure. This is further evidence that the acoustic signal cannot be used to estimate the pressure impulse. The flash photographs also confirm that the bubble sizes are quite similar for the contact and noncontact delivery in those experiments.

The bubble energy increases with increasing laser-pulse energy for both contact and noncontact delivery (Fig. 7). However, conversion efficiency of laser-pulse energy into cavitation bubble energy is slightly greater for contact delivery (6%) than for noncontact delivery (4%). This may be the reason that the pressure impulses generated by contact delivery are always greater than those generated by noncontact delivery when the same energy is used. Thus the mode of light delivery (contact versus noncontact) plays only an indirect role for the pressure-impulse generation.

Note that only a small fraction (4–6%) of the laser-pulse energy is converted into the bubble energy, the pressure–volume work done by the bubble. Such low conversion efficiencies of the pulse energy into the bubble have also been reported by other investigators. Vogel *et al*. estimated a large range of bubble energies between 1% and 25% of the laser pulse energies during intraocular surgery.[20–22] The bubbles were generated by laser-induced breakdown by using picosecond and nanosecond laser pulses. A study by Rink *et al*. reported that the conversion efficiency was up to 30% during laser lithotripsy with a 2.5-μs pulsed-dye laser.[2] The conversion efficiency seems to depend on pulse duration, energy, and irradiation target. However, by using the Rayleigh formula, one cannot determine how much of the pulse energy goes into the initial pressure transients and how much is wasted as heat.

Only ~10–15% of the bubble energy contributes to the generation of pressure impulses. It is unclear what happens to the bulk of the bubble energy, but much is likely lost through heating, acoustic radiation, resistance from the gelatin sample, and reflection at boundaries because of impedance mismatch. By conservation of momentum, the momentum carried by the collapsing cavitation bubble must be equal to the sum of the pressure impulse and the momentum associated with the material ejection from the gelatin surface. However, the techniques used in this study are not able to distinguish those differences. Thus we are reporting part of the momentum transfer story but not, for example, quantifying such parameters as pressure amplitude and duration.

This study has shown that no displacement of the cuvette occurs when the cuvette does not contact the metal plate. This result is most likely because in this case no momentum can be reflected from the rigid metal plate. It is also observed that the displacement of the cuvette decreases dramatically when a soft material, e.g., tissue paper, is put between the bottom of the cuvette and the metal plate. Similar effects are observed during the tube experiments. This emphasizes that the pressure impulses would not cause target rebound as long as there is no hard boundary to cause reflection of the momentum. However, the surface of the water contained in the cuvette vibrates in both cases, presumably as a result of internal fluid motion associated with the bubble expansion and collapse.

The results of the tube experiments reveal that the pressure impulses propagate both axially and radially, but the tendency for the tube to be displaced in the radial direction appears to be much less than that in the axial direction (i.e., the direction of the laser-pulse delivery). This phenomenon may be caused by the asymmetrical boundaries in both axial and radial directions. We speculate that the bubble causes a Kelvin impulse due to the Bjerknes force that is created by the pressure gradient normal to the boundary (in our case, the metal plate) during its collapse.

The jet passes through the bubble away from the boundary, and an oppositely directed pressure impulse travels across the boundary. Eventually, the reflected pressure causes the tube to rebound. The displacement is less in the radial direction, which implies that asymmetries in the radial direction are weaker than in the axial direction.

The light-delivery fiber may sometimes be in direct contact with the vessel wall *in vivo* because of the difficulty of precisely positioning the fiber-optic catheter. However, the pressure impulses would still be unlikely to lead to vessel perforation because usually no hard boundary stands behind the arterial wall. However, van Leeuwen *et al*. demonstrated that some tissue elevation may occur when the fiber tip is in contact with porcine aorta submerged in saline with a 500-mJ holmium laser pulse.[12] They also suggest that dissection may result from *in vivo* bubble expansion. It remains to be investigated whether or not the pressure impulses can cause perforation or dissection *in vivo*. It is not clear whether the internal fluid motion revealed by the surface vibration could cause a net displacement of the catheter, but our experiments suggest that this would be a much smaller effect than the displacement associated with a reflecting surface.

5. Conclusion

This study has demonstrated that the pressure impulses occurring in laser thrombolysis strongly depend on the energy stored in the cavitation bubble regardless of the light-delivery method (contact versus noncontact) and that the resulting impulses are not directly correlated with the acoustic transients. The pressure impulses do seem to be associated with the bubble-driven jet formation due to the bubble collapse. Significant rebound of the ablation targets occurs only when the target is supported by a hard boundary. It is unlikely that the rebound of thrombus due to pressure impulses would cause the surrounding vessel to jump so much that the catheter would impinge on it, since the obstructed vessels are usually surrounded by soft tissues in most cardiovascular applications. *In vivo* experiments may be desirable for further clarification of this matter.

We thank K. W. Gregory and A. Shearin for generous support of this project and R. P. Godwin of Los Alamos National Laboratory for useful discussions. This research was supported in part by the Murdock Foundation, Portland, Ore., and the Whitaker Foundation, Washington, D.C.

References

1. A. Vogel and W. Lauterborn, "Acoustic transient generation by laser-produced cavitation bubbles near solid boundaries," J. Acoust. Soc. Am. **84,** 719–731 (1988).
2. K. Rink, G. Delacrétaz, and R. P. Salathé, "Fragmentation process of current laser lithotriptors," Lasers Surg. Med. **16,** 134–146 (1995).
3. E. D. Jansen, T. Asshauer, M. Frenz, M. Motamedi, G. Delacrétaz, and A. J. Welch, "Effect of pulse duration on bubble formation and laser-induced pressure waves during holmium laser ablation," Lasers Surg. Med. **18,** 278–293 (1996).
4. T. G. van Leeuwen, E. D. Jansen, A. J. Welch, and C. Borst, "Excimer laser induced bubble: dimensions, theory, and implications for laser angioplasty," Lasers Surg. Med. **18,** 381–390 (1996).
5. K. Gregory, "Laser thrombolysis," in *Interventional Cardiology*, vol. 2, E. J. Topol, ed. (Saunders, Philadelphia, Pa., 1994), pp. 892–902.
6. F. Litvack, "Excimer laser coronary angioplasty," in *Interventional Cardiology*, vol. 2, E. J. Topol, ed. (Saunders, Philadelphia, Pa., 1994), pp. 841–866.
7. O. Topaz, "Holmium:YAG coronary angioplasty: the multicenter registry," in *Interventional Cardiology*, vol. 2, E. J. Topol, ed. (Saunders, Philadelphia, Pa., 1994), pp. 867–891.
8. H. Shangguan, L. W. Casperson, and S. A. Prahl, "Microsecond laser ablation of thrombus and gelatin under clear liquids: contact versus non-contact," IEEE J. Selec. Topics Quantum Electron. **2,** 818–825 (1996).
9. T. Tomaru, H. J. Geschwind, G. Boussignac, F. Lange, and S. J. Tahk, "Characteristics of shock waves induced by pulsed lasers and their effects on arterial tissue: comparison of excimer, pulse dye, and holmium YAG lasers," Am. Heart J. **123,** 896–904 (1992).
10. H. Shangguan, L. W. Casperson, A. Shearin, K. W. Gregory, and S. A. Prahl, "Drug delivery with microsecond laser pulses into gelatin," Appl. Opt. **35,** 3347–3357 (1996).
11. R. de la Torre and K. W. Gregory, "Cavitation bubbles and acoustic transients may produce dissections during laser angioplasty," J. Am. Coll. Cardiol. **19A,** 48 (1992).
12. T. G. van Leeuwen, L. van Erven, J. H. Meertens, M. Motamedi, M. J. Post, and C. Borst, "Original of arterial wall dissections induced by pulsed excimer and mid-infrared laser ablation in the pig," J. Am. Coll. Cardiol. **19,** 1610–1618 (1992).
13. T. G. van Leeuwen, J. H. Meertens, E. Velema, M. J. Post, and C. Brost, "Intraluminal vapor bubble induced by excimer laser pulse causes microsecond arterial dilation and invagination leading to extensive wall damage in the rabbit," Circulation **87,** 1258–1263 (1993).
14. P. A. Tipler, *Physics for Scientists and Engineers*, vol. 1, (Worth, New York, 1990), p. 210.
15. Lord Rayleigh, "On the pressure developed during the collapse of a spherical cavity," Philos. Mag. **34,** 94–98 (1917).
16. A. Vogel, R. Engelhardt, U. Behnle, and U. Parlitz, "Minimization of cavitation effects in pulsed laser ablation—illustrated on laser angioplasty," Appl. Phys. B **62,** 173–182 (1996).
17. T. B. Benjamin, B. B. Taib, and A. T. Ellis, "The collapse of cavitation bubbles and the pressures thereby produced against solid boundaries," Philos. Trans. R. Soc. London Ser. A **260,** 221–240 (1966).
18. J. R. Blake, B. B. Taib, and G. Doherty, "Transient cavities near boundaries. part 1: rigid boundary," J. Fluid Mech. **170,** 479–497 (1986).
19. E. J. Chapyak, R. P. Godwin, S. A. Prahl, and H. Shangguan, "A comparison of numerical simulations and laboratory studies of laser thrombolysis," in *Lasers in Surgery: Advanced Characterization, Therapeutics, and Systems VII*, R. R. Anderson, K. E. Bartels, L. S. Bass, K. W. Gregory, D. M. Harris, H. Lui, R. S. Malek, G. J. Mueller, M. M. Pankratov, A. P. Perlmutter, H. Reidenbach, P. L. Tate, and G. M. Watson, eds., Proc. SPIE **2970,** 23–34 (1997).
20. A. Vogel, W. Hentschel, J. Holzfuss, and W. Lauterborn, "Cavitation bubble dynamics and acoustic transient generation in ocular surgery with pulsed neodymium:YAG lasers," Ophthalmology **93,** 1259–1269 (1986).
21. A. Vogel, P. Schweiger, A. Frieser, M. N. Asiyo, and R. Birngruber, "Intraocular Nd:YAG laser surgery: Light-tissue interaction, damage range, and reduction of collateral effects," IEEE J. Quantum Electron. **26,** 2240–2259 (1990).
22. A. Vogel, S. Busch, K. Jungnickel, and R. Birngruber, "Mechanisms of intraocular photodisruption with picosecond and nanosecond laser pulses," Lasers Surg. Med. **15,** 32–43 (1994).